J Fluoresc
DOI 10.1007/s10895-008-0362-x

ORIGINAL PAPER

A Fluorescent and Phosphorescent Nanoporous Solid: Crystalline Calix[4]arene

Issam Oueslati · Anthony W. Coleman · Baltazar de Castro · Mário N. Berberan-Santos

Received: 6 February 2008 / Accepted: 10 March 2008

Abstract Calix[4]arene forms elongated nanoporous microcrystals. The pores are linear nano-channels (1.7 nm diameter) arranged in a honeycomb network. The crystals luminesce at room temperature according to a variety of processes that include monomer fluorescence (lifetime of ca. 1.1 ns), dimer fluorescence (lifetime of ca. 5.4 ns), and monomer phosphorescence (lifetime of ca. 2 s). The dimers result from π-orbital overlap of adjacent phenol groups from neighboring nano-channels, with C–C distances of ca. 4 Å.

Keywords Calixarene · Nano-channel · Room-temperature phosphorescence · Luminescent dimer

Introduction

Organic and inorganic nanotubes are of great importance in nanotechnology [1, 2]. The closely related supramolecular architectures with tubular morphologies are also of interest in materials science, biomimetic chemistry, and molecular electronics [3–6]. The rigid skeleton of calixarenes allowed the design of a few tubular systems including *p*-sulfonated, methoxycarboxylic acid, hydroxyphosphonic acid and hydroquinone derivatives of calixarene [7–11]. The tubes are either filled with guest entities or interconnected by bridging water molecules. Recently, we reported a pure organic crystalline solid assembled from a distal calix[4]arene dimethylester derivative **1** (cf. Fig. 1) in which hydrogen bonds and van der Waals interactions gave rise to a stable linear nanoscale tubular polymeric structure with repeating tubular hexamer units [12].

In the present work we investigate the luminescence properties of these nanoporous crystals. The photophysical study was performed by UV-absorption spectroscopy, and fluorescence and phosphorescence spectroscopies in solution and in the solid state at different temperatures, while scanning electron microscopy (SEM) was used to elucidate the solvent effect on crystal morphology.

Experimental

Materials Acetonitrile was of spectroscopic grade from Aldrich. Dichloromethane, chloroform, methanol and diethyl ether were of reagent grade quality. Compound **1** was prepared following a previously described procedure and the crystals used were grown from a chloroform/methanol mixture [12].

Microscopic characterization The crystal suspensions were dropped on a stub and coated, after drying, with a gold layer, then observed under a scanning electron microscope Hitachi S-2400 with Rontec standard EDS detector.

Spectroscopic measurements All UV spectroscopic measurements were performed with a Shimadzu UV-3101PC UV-vis-NIR spectrometer at 293 K equipped with MPC-

I. Oueslati (✉) · M. N. Berberan-Santos
Centro de Química-Física Molecular, Instituto Superior Técnico,
Av. Rovisco Pais,
1049-001 Lisboa, Portugal
e-mail: issam.oueslati@ist.utl.pt

A. W. Coleman
IBCP (CNRS UMR 5086),
7 passage du Vercors,
F-69367 Lyon, France

B. de Castro
Departamento de Química, Universidade do Porto,
Rua Campo Alegre,
4169-007 Porto, Portugal

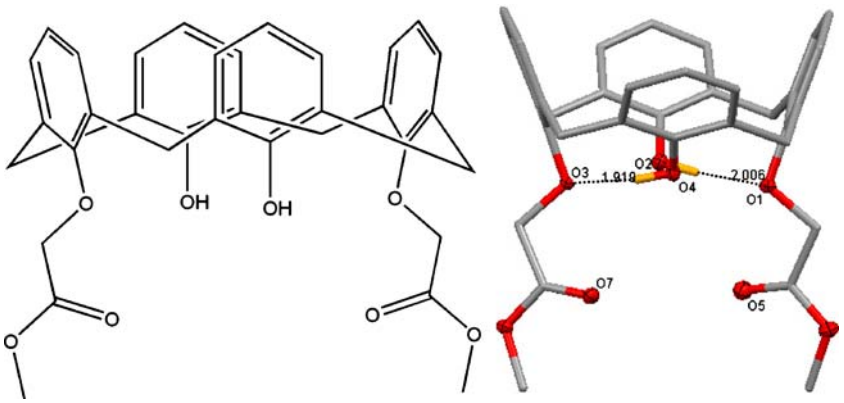

Fig. 1 Molecular structure of **1** (*left*) and the crystal structure of its monomer (*right*). Hydrogen bonds are shown as *black dashed lines*

3100 apparatus for solid state measurements and with cells of 1.0 cm optical path length for solution measurements. Measurements of the calixarene emission (fluorescence and phosphorescence) were carried out at 293 K with a Fluorolog Spex F112A fluorimeter and corrected for instrumental response. Right angle configuration was adopted to record emission spectra in solution, using 1.0 cm path length cells. Crystals of **1** were melted between two quartz surfaces and their emission spectra were recorded in a front face configuration. The fluorescence quantum yield of calixarene was determined using an optically matched solution (OD ca. 0.1) of phenol (Φ_F=7.5% in *n*-hexane [13]) as standard. Time resolved picosecond fluorescence intensity decays were obtained by the single-photon timing method with laser excitation. The set-up consisted of a mode-locked Coherent Innova 400-10 argon-ion laser that synchronously pumped a cavity dumped Coherent 701-2 dye laser, delivering 3–4 ps pulses (with ca. 40 nJ/pulse) at a frequency of 3.4 MHz. Intensity decay measurements were made by alternated collection of impulse and decays with the emission polarizer set at the magic angle position. Impulse was recorded slightly away from excitation wavelength with a scattering suspension. For the decays, a cut-off filter was used, effectively removing all excitation light. Detection was always done by passing the emission through a depolarizer and then through a Jobin-Yvon HR320 monochromator with a grating of 100 lines/mm. Usually no less than 5,000 counts were accumulated at the maximum channel. The detector employed was a Hamamatsu 2809U-01 microchannel plate photomultiplier. The instrument response function had an effective FWHM of 35 ps. Decay data analysis was performed with the Globals Unlimited software package (Laboratory for Fluorescence Dynamics, University of Illinois, USA).

Results and discussion

Hexagonal self-assembly of calixarene monomers Calix[4]arene 1,3-di-methoxycarbonylmethoxy **1**, Fig. 1, was prepared by treatment of calix[4]arene with methyl bromoacetate in refluxing acetone, in the presence of K_2CO_3. Diffraction quality single crystals of **1** [trigonal space group R-3] were obtained from a dichloromethane/methanol or chloroform/methanol solution, or chloroform/diethyl ether or chloroform/water solution. Contrary to analogous disubstituted calix[4]arenes adopting a dimeric pattern [9, 11, 14–16], **1** is present as a monomer motif (cf. Fig. 1). The designed *flattened cone* conformation is relatively similar to what was observed for diethylester calix[4]arenas [17–20] and less distorted than observed for calix[4]arenes disubstituted with other functional groups [9, 11, 21, 22].

The self-assembly of calixarene monomers of **1** leads to a regular hexagonal nanoporous architecture with linear tubular cavities of approximately 1.7 nm of diameter (cf. Fig. 2 left). The supramolecular sextet units are arranged into a regular hexagon with an inner angle of 115°. The hexagonal architecture is in turn assembled into discrete honeycomb structures of 5.2 nm size that are occasionally observed with calix[4]arenes (cf. Fig. 2 right) [7, 9, 11]. X-Ray diffraction studies revealed that whatever the solvent mixture used in the crystallization procedure, the honeycomb assembly is always observed. The interactions between neighboring nanotubes are comparable to recent observations for the self-assembly of di-methoxycarboxylic acid derivative of calix[4]arene, [11] and are formed by intermeshing gear type contacts generated by the interdigitation of the aromatic rings (cf. Fig. 2 right).

Solvent effect on the crystal habit SEM images obtained show dissimilarities in crystal morphology dependent on modification of the solvent mixture. Crystals with irregular shape are obtained in chloroform/water, however the hexagonal structure (regular shape) is only seen for crystals grown in chloroform/methanol or chloroform/diethyl ether. Further, the crystal-size decreases when going from methanol to diethyl ether and water. The crystal habit results from the relative growth rates of its surfaces in different directions [23]. Therefore, preferential growth or inhibition of different

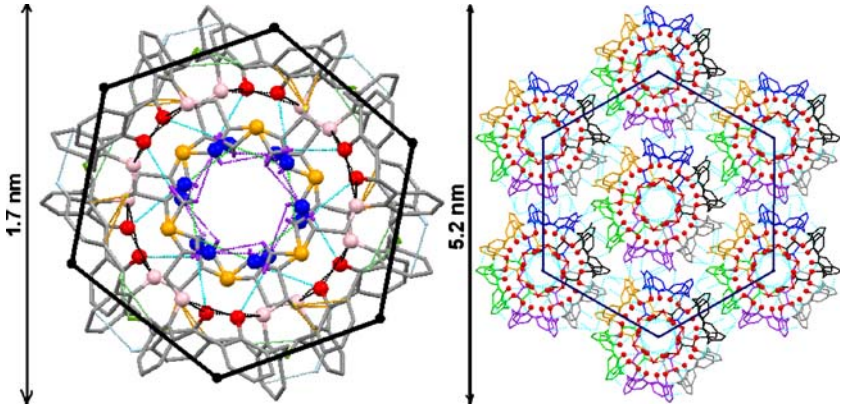

Fig. 2 View down the *c* axis of the fundamental supramolecular unit (*left*) and the molecular interactions generating the honeycomb structure (*right*)

crystal faces changes the shape of the crystal. The solvent effect on the growth rate of the various crystal habit faces has been evidenced [24–26]. Further, the energy barrier for particle aggregation is significantly dependent on the dielectric constant of the solvent mixture, and it seems that the increase of the dielectric constant produces irregular aggregates, however the decrease of this parameter produces soft agglomerates [27]. This, in turn, could explain the observed morphologies of **1** since the dielectric constant decreases from water (80) to methanol (33) and diethyl ether (4.3). The visual evidence of the formation of the nanotubular assemblies generated by a linear network of microscale tubes of 17.95 μm size which could correspond to a cluster of ca. 3,500 hexagonal supramolecular units is shown in Fig. 3. The inner angle of the hexagonal bundle (cf. Fig. 3 right) is relatively similar to that determined for the hexagons in the honeycomb structure (see above) i.e. 121° against 115°. As the crystal growth in chloroform/diethyl ether was mostly achieved along the *c* axis, it is anticipated that the prepared crystals are very anisotropic.

Photophysics of 1 in solution and in the crystalline state The UV absorption spectra of **1** dissolved in acetonitrile (1.4×10^{-4} M) consists of two broad bands similar to those observed for calix[4]- and [6]arenes, and for monomeric methoxybenzenes [28–31]. These absorption bands correspond to the first π,π^* transitions of the aromatic moiety. The strong band at 210 nm (ε=11,000 L mol^{-1} cm^{-1}) is the perturbed L_a transition of benzene, while the weaker band between 250 and 300 nm with a maximum at 280 nm (ε= 6,000 L mol^{-1} cm^{-1}) is the perturbed L_b transition of benzene (cf. Fig. 4 left) [32]. In the crystal, the latter band is broader (200 to 320 nm) and displays two closely spaced peaks at 273 nm and 283 nm, cf. Fig. 4 left. This band splitting is assigned to dimer formation between aryl groups from neighboring monomers in the crystal, as will be discussed below.

In a dilute acetonitrile solution, the emission spectrum of **1** is broad and structureless (cf. Fig. 4 right) with a maximum at 307 nm. A mirror correspondence of absorption and fluorescence is observed and the excitation spectrum closely resembles the absorption one. The emission quantum yield is Φ_F=0.29 and the decay is single exponential, with a lifetime τ=1.9 ns. This emission is therefore the fluorescence of the aryl moieties. The luminescence spectrum of **1** in the crystal lattice is much more complex (Fig. 4 right). It shows, besides the strong 308 nm band (two-exponential decay with lifetimes 0.21 and 0.66 ns, with an average

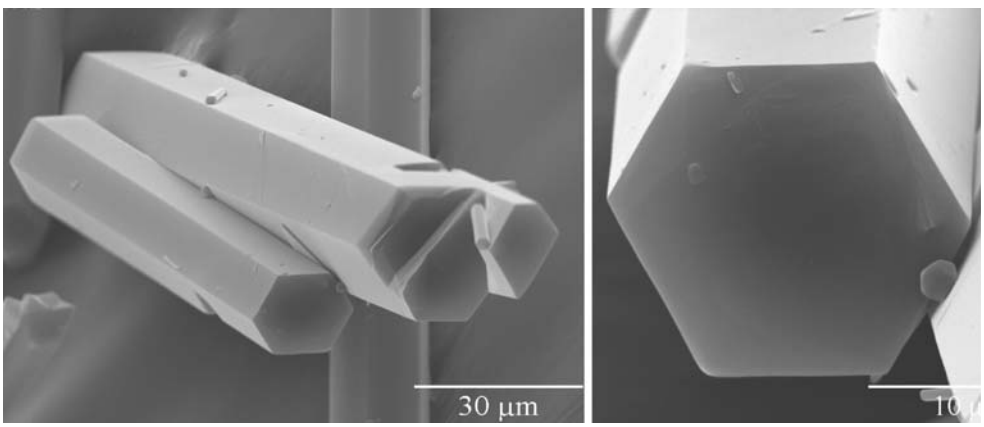

Fig. 3 SEM images of the microcrystalline hexagonal assembly of **1** (*left*: ×1,000, *right*: ×4,000)

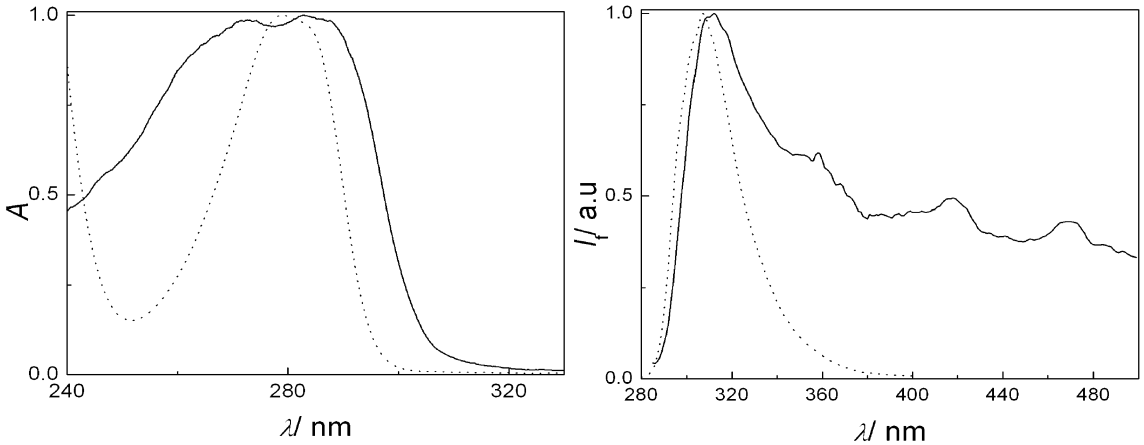

Fig. 4 Normalized absorption (*left*) and luminescence (*right*) spectra of **1** (1.4×10^{-4} M) in acetonitrile (*dotted line*) and in the crystal form (*full line*)

fluorescence lifetime $<\tau>=0.49$ ns) and originating from the monomer, three more bands at 360, 416, and 467 nm. For the larger 4-sulfonated calix[6]arene, which bears a related fluorophore (with a supplementary SO_3^- group in *p*-position), Zhang et al. [31] ascribed the intramolecular low energy emission band to excimer emission (excited state association of two phenol groups). In our case the structured emission observed, with three maxima, is not compatible with the exclusive presence of excimer emission, which is structureless owing to the dissociative nature of the ground state. Low temperature, lifetime and anisotropy measurements show that this assignment is indeed not correct for the 416 nm and 467 nm bands: We recorded the luminescence spectra of an acetonitrile solution of 2,6-dimethylanisole (1.4×10^{-4} M), at room temperature and at 77 K. The monomer fluorescence band at 308 nm is present in both spectra, while the 416 and 467 nm bands appear only at 77 K. The emission spectrum at 77 K recorded with a delay of a few ms displays exclusively the latter two bands which are, therefore, assigned to phosphorescence of the aromatic moiety. The respective luminescence decays are monoexponential with lifetimes of ca. 2–3 s, and are very close to the phosphorescence lifetimes of phenol (2.9 s) and anisole (3.0 s) [33]. As expected, the phosphorescence is observed solely at low temperature or in the solid state where oxygen quenching is prevented. The 416 and 467 nm bands in the luminescence spectrum of the crystal are thus due to phosphorescence originating from both monomer (aryl moiety) and dimers, since excitation of the crystal above 300 nm, where the monomer does not absorb, still yields the 416 and 467 nm bands.

Steady-state emission anisotropy spectra of both the crystal and a rigid solution of **1** (cf. Fig. 5) show negative anisotropy values for the 416 and 467 nm bands confirming that these correspond to phosphorescence, whose transition moments are out-of-plane in aromatic molecules.

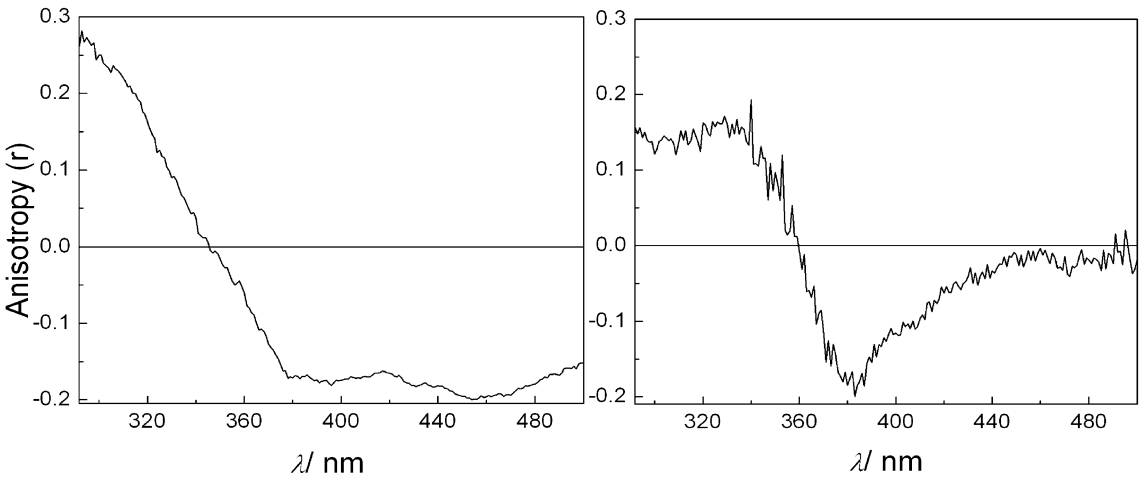

Fig. 5 Steady-state emission anisotropy spectra of **1** in the crystalline form (*left*, at 293 K) and in a low temperature glass [toluene–methylcyclohexane (1:4); (*right*)]. Excitation wavelength=267 nm

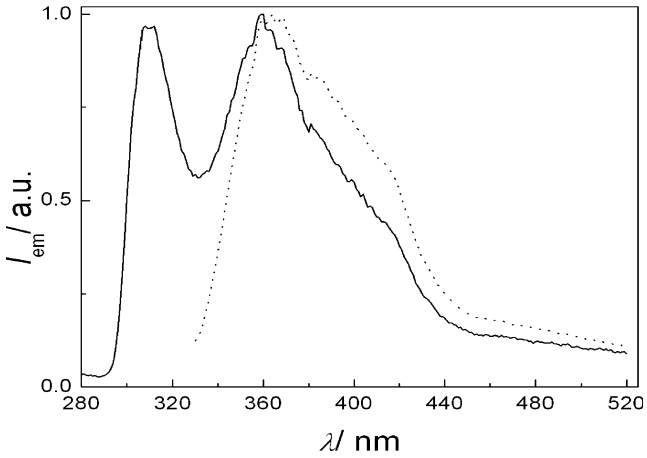

Fig. 6 Normalized fluorescence (*dotted line* λ_{exc}=320 nm, and *full line* λ_{exc}=267 nm) spectra of **1**, 1.4×10^{-2} M in acetonitrile

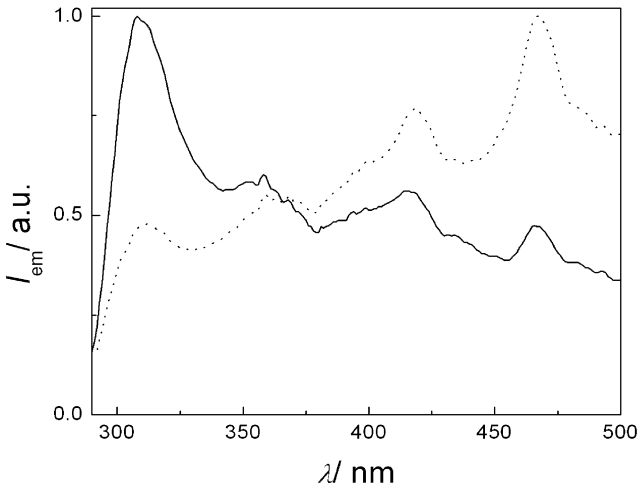

Fig. 8 Fluorescence spectra of **1,** 1.4×10^{-4} M in acetonitrile (*dotted line*, at 230 K) and in the crystal form (*full line*, at 296 K)

With respect to the 360 nm band observed in the crystal (two-exponential decay with lifetimes 1.1 and 5.4 ns, with an average fluorescence lifetime $<\tau>$=2.1 ns) it is not clear from spectral data whether it mainly results from a preformed excimer or from a ground state dimer, the distinction between the two possibilities being a subtle one. To better assign this band, we measured the fluorescence spectra of a concentrated solution of **1** (cf. Fig. 6) upon excitation at 267 nm and also at 320 nm (where the monomer does not absorb).

The first emission band at 308 nm corresponds to the monomer fluorescence, but the additional broad band centered at 360 nm results from the fluorescence of a dimer since it is still observed upon excitation at 320 nm. This is further evidenced by the marked increase of the fluorescence intensity ratio I(360 nm)/I(308 nm) when going from 10^{-4} to 10^{-2} M, resulting from shifting the monomer-dimer equilibrium. Interestingly, the 360 nm band is present in the fluorescence spectrum of the tetra-methylester substituted calix[4]arene but not in the fluorescence spectrum of the parent compound (with four hydroxyl groups), showing, therefore, that the 360 nm band in the fluorescence spectrum of the crystal arises from interactions between adjacent phenol groups through π-orbital overlap. These phenol groups have a C–C (centroid–centroid) distance of 3.94 Å, and come from neighboring supramolecular units in the crystal lattice (cf. Fig. 7 middle and right). Such a parallel-displaced structure is usually observed and has a contribution from π–σ attraction [34].

The existence of ground state dimers is further documented by the already mentioned splitting observed in the L_b absorption band (cf. Fig. 4 left) [35]. The fluorescence decay measured at 360 nm contains, as mentioned, a long lifetime component of 5.4 ns (ca. 25% of the total intensity), tentatively assigned to the dimer. The shorter lifetime component (1.1 ns) is assigned to the monomer emission in the crystal, as it is comparable to the 1.9 ns lifetime of the calixarene in solution. The pronounced red-shift of ca. 52 nm in the fluorescence emission of the dimer, as compared to the monomer emission, indicates strong coupling between the aromatic rings and is characteristic of molecules which crystallize with a lattice type similar to that of pyrene or perylene [36, 37]. Ferguson et al. interpreted this displacement as a charge-transfer transition involving the pyrene

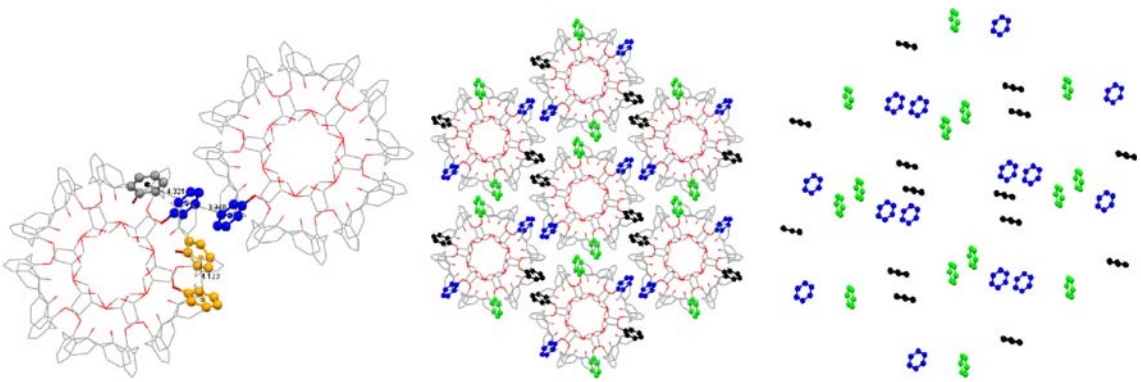

Fig. 7 View (*left*) of the expected interacting phenols and (*middle and right*) of the overlapping parallel phenols

molecules grouped in pairs in the crystal [38]. The phenol groups in the calixarene rings, supporting the pendant arms and making a dihedral angle of 21.59° with the symmetry plane passing through the two flattened phenols, are arranged along three distinct directions (black, blue and green in Fig. 7 right) with a similar interplanar angle of 76.2°.

The temperature dependence of fluorescence was also investigated in the solid state and in solution. The fluorescence spectrum of the crystal does not change significantly upon heating. On the other hand, the cooling of an acetonitrile solution of **1** leads to significant changes in the fluorescence spectrum, with the appearance of the dimer fluorescence band (below 260 K) and of two phosphorescence bands at low temperature (negative anisotropy values above 400 nm, Fig. 5 right). The fluorescence spectrum of **1** in the low temperature rigid glass (cf. Fig. 8) thus resembles that of the crystal at room temperature, indicating that the calixarene molecules aggregate or crystallize.

Conclusions

In summary, we have prepared phosphorescent microscale bundles of calix[4]arene nano-channels, assembled in a honeycomb structure, with hydrophobic outer-surface and hydrophilic inner-surface, and characterized them by SEM and absorption and luminescence studies. The prepared crystals are highly anisotropic. The strength of the intramolecular hydrogen bonds and the geometry of the pendant arms along with intermolecular short contacts are significant factors for the stability of the tubular architecture. SEM investigations show a solvent effect on the crystal habit and validate the hexagonal self-assembly. The fluorescence spectrum of the crystal results in part from a strong coupling between aromatic rings from adjacent supramolecular units, leading to the formation of ground state dimers. The long-lived phosphorescence is observed in solution at low temperature and in the crystal at all temperatures.

Acknowledgment This work was supported by the Portuguese Foundation for Science and Technology (Project POCI/QUI/58535/2004 and a postdoctoral grant SFRH/BPD/14593/2003).

References

1. Zaworotko MJ (2000) Nanoporous structures by design. Angew Chem Int Ed 39(17):3052–3054
2. Fenniri H, Mathivanan P, Vidale KL, Sherman DM, Hallenga K, Wood KV, Stowell JG (2001) Helical rosette nanotubes: design, self-assembly, and characterization. J Am Chem Soc 123:3854–3855
3. Firouzi A, Kumar D, Bull LM, Besier T, Sieger P, Huo Q, Walker SA, Zasadzinski JA, Glinka C, Nicol J (1995) Cooperative organization of inorganic-surfactant and biomimetic assemblies. Science 267:1138–1143
4. Vreekamp RH, van Duynhoven JPM, Hubert M, Verboom W, Reinhoudt DN (1996) Molecular boxes based on calix[4]arene double rosettes. Angew Chem Int Ed Engl 35:1215–1218
5. Zimmerman SC, Zeng F, Reichert DEC, Kolotuchin SV (1996) Self-assembling dendrimers. Science 271:1095–1098
6. Atwood JL, Barbour LJ, Jerga A (2002) Storage of methane and freon by interstitial van der Waals confinement. Science 296:2367–2369
7. Orr GW, Barbour LJ, Atwood JL (1999) Controlling molecular self-organization: formation of nanometer-scale spheres and tubes. Science 285:1049–1052
8. Hong BH, Lee JY, Lee C-W, Kim JC, Bae SC, Kim KS (2001) Self-assembled arrays of organic nanotubes with infinitely long one-dimensional H-bond chains. J Am Chem Soc 123:10748–10749
9. Coleman AW, Da Silva E, Nouar F, Nierlich M, Navazar A (2003) The structure of a self-assembled calixarene aqua-channel system. Chem Commun 7:826–827
10. Tedesco C, Immediata I, Gregoli L, Vitagliano L, Immirzi A, Neri P (2005) Interconnected water channels and isolated hydrophobic cavities in a calixarene-based, nanoporous supramolecular architecture. CrystEngComm 7(73):449–453
11. Lazar AN, Dupont N, Navazar A, Coleman AW (2006) Helical aquatubes of calix[4]arene di-methoxycarboxylic acid. Chem Commun 1076–1078
12. Perret F, Lazar AN, Shkurenko O, Suwinska K, Dupont N, Navazac A, Coleman AW (2006) Geometrical and inclusion considerations in the formation of hexagonal nanotubes of calix[4]arene di-methoxycarbonyl methyl ester and acid. CrystEngComm 8:890–894
13. Grabner G, Kohler G, Marconi G, Monti S, Venuti E (1990) Photophysical properties of methylated phenols in nonpolar solvents. J Phys Chem 94:3609–3613
14. Lipkowski J, Simonov Y, Kalchenko VI, Vysotsky MA, Markovsky LN (1998) Molecular and crystal structure of water-soluble 25,27-bis(dihydroxyphosphoryloxy)-calix[4]arene. An Quim Int Ed 94:328–331
15. Lui Y, Huang G, Zhang H-Y (2002) Synthesis and crystal structure of 26,28-bis(cyanomethoxy)-25,27-dihydroxycalix[4]arene. J Mol Struct 608:213–217
16. Kuzmina LG, Sadikov GG, Howaed JA, Shokova EA, Kovalev VV (2003) Molecular and crystal structures of calix[4]arene 1,3-di-*n*-propyl ether. Crystallogr Rep 48:233–238
17. Coles SJ, Hall CW, Hursthouse MB (2002) 2,4-Dihydroxy-1,3-bis(methoxycarbonylmethoxy)calix[4]arene and 1,3-bis(ethoxycarbonylmethoxy)-2,4-dihydroxycalix[4]arene chloroform solvate. Acta Crystallogr, Sect. C: Cryst Struct Commun 58:o29–o31
18. Dudi M, Lhoták P, Petíková H, Stibor I, Lang K, Sýkora J (2003) Calixarene-based metalloporphyrins: Molecular tweezers for complexation of DABCO. Tetrahedron 59:2409–2415
19. Genorio B, Kobe J, Giester G, Leban I (2003) Cone and 1,3-alternate conformers of 1,3-bis(ethoxycarbonylmethoxy)-2,4-dihydroxycalix[4]arene and 1,2,3,4-tetrakis(ethoxycarbonylmethoxy)calix[4]arene. Acta Crystallogr, Sect.C: Cryst Struct Commun 59:o221–o224
20. Liu H, Li B, Liu Y, Xu Z (2003) Two novel self-assemblies of the calix[4]arene derivatives and their structures. J Incl Phenom 45:9–11
21. Beer PD, Drew MGB, Gradwell K (2000) Synthesis and anion coordination chemistry of new calix[4]arene pyridinium receptors. J Chem Soc, Perkin Trans 2:511–519
22. Lazar AN, Navaza A, Coleman AW (2004) Solid-state caging of 1,10-phenanthroline p-p stacked dimers by calix[4]arene dihydroxyphosphonic acid. Chem Commun 1052–1053
23. Hartman P, Bennema P (1980) The attachment energy as a habit controlling factor: I. Theoretical considerations. J Cryst Growth 49:145–156

24. Song X, Sun S, Fan W, Yu H (2003) Preparation of different morphologies of calcium sulfite in organic media. J Mater Chem 13:1817–1821
25. Arslantas A, Ermler WC, Yazici R, Klyon DM (2004) Crystal habit modification of vitamin C (L-ascorbic acid) due to solvent effects. Turk J Chem 28:255–270
26. Stoica C, Verwer P, Meekes H, van Hoof PJCM, Kaspersen FM, Vlieg E (2004) Understanding the effect of a solvent on the crystal habit. Cryst Growth Des 4:765–768
27. Hua Z, Wang XM, Xiao P, Shi J (2006) Solvent effect on microstructure of yttria-stabilized zirconia (YSZ) particles in solvothermal synthesis. J Eur Ceram Soc 26:2257–2264
28. Prodi L, Bolletta F, Montalti M, Zaccheroni N, Casnati A, Sansone F, Ungaro R (2000) Photophysics of 1,3-alternate calix [4]arene-crowns and of their metal ion complexes: evidence for cation-p interactions in solution. New J Chem 24:155–158
29. de María Ramírez F, Charbonnière L, Muller G, Scopelliti R, Bünzli J-CG (2001) A *p-tert*-butylcalix[4]arene functionalised at its lower rim with ether-amide pendant arms acts as an inorganic-organic receptor: structural and photophysical properties of its lanthanide complexes. J Chem Soc, Dalton Trans 21:3205–3213
30. Oueslati I, Sá Ferreira RA, Carlos LD, Baleizão C, Berberan-Santos MN, de Castro B, Vicens J, Pischel U (2006) Calix[4]azacrowns as novel molecular scaffolds for the generation of visible and near-infrared lanthanide luminescence. Inorg Chem 45:2652–2660
31. Zhang Y, Agbaria RA, Mukundan NE, Warner IM (1996) Spectroscopic studies of water-soluble sulfonated calix[6]arene. J Incl Phenom Mol Recognit Chem 24:353–365
32. Jaffé HH, Orchin M (1962) Theory and applications of ultraviolet spectroscopy. Wiley, New York, xv + 624 pp
33. McClure DS (1949) Triplet-singlet transitions in organic molecules. Lifetime measurements of the triplet state. J Chem Phys 17:905–913
34. Janiak C (2000) A critical account on p–p stacking in metal complexes with aromatic nitrogen-containing ligands. J Chem Soc, Dalton Trans 21:3885–3896
35. Cantor CR, Schimmel PR (1980) Biophysical chemistry part II: Techniques for the study of biological structure and function. W. H. Freeman and Company, Oxford
36. Stevens B (1962) Some effects of molecular orientation on fluorescence emission and energy transfer in crystalline aromatic hydrocarbons. Spectrochim Acta 18:439–448
37. Simpson WT, Peterson DL (1957) Coupling strength for resonance force transfer of electronic energy in van der Waals solids. J Chem Phys 26:588–593
38. Ferguson J (1958) Absorption and fluorescence spectra of crystalline pyrene. J Chem Phys 28:765–768